

# Indoor Scene Intelligent Identification System Based on Spatial Topological Relationship Constraints

Shenglei Xu<sup>1</sup>, Yaqin Sun<sup>2</sup>

<sup>1</sup> Navigation Institute of Jimei University, Xiamen, Fujian Province, China – [jmu-xsl@jmu.edu.cn](mailto:jmu-xsl@jmu.edu.cn)

<sup>2</sup> School of Environmental Science and Spatial Informatics, China University of Mining and Technology, Xuzhou, Jiangsu Province, China – [syqin@cumt.edu.cn](mailto:syqin@cumt.edu.cn)

**Keywords:** Indoor Scene Identification, Spatial Topology, Indoor Positioning, Intelligent System.

## Abstract

Indoor scene identification can provide prior environmental information for indoor positioning applications, achieving positioning enhancement. Due to the similarity of wireless signals in adjacent spaces, it can lead to incorrect identification in neighbouring scenario units. To address this problem, this paper first employs a Naive Bayes classifier to train and classify wireless signal strength data from different scenes, constructing a scene identification algorithm. Secondly, a topological relationship adjacency matrix and adjacency list tailored for indoor positioning are constructed, imposing spatial topological constraints to assist scene identification. Finally, an indoor scene intelligent identification system is developed and implemented. The experimental results indicate that the scene identification method based on spatial topological relationship constraints can effectively improve identification accuracy. The overall accuracy for 8 scenario units is 98.2%, and the identification accuracy is increased by 1.1% compared with the original method.

## 1. Introduction

In recent years, with the development of Internet of Things (IoT), indoor positioning technology has become important in many fields such as indoor navigation, context awareness, smart logistics, emergency rescue and so on (Obeidat et al., 2021). Indoor positioning is closely related to indoor scenes, which are characterized by complex spatial structures and diverse building materials, profoundly affecting the propagation of various wireless signals. Utilizing environment information to enhance indoor scene perception and identification, and achieving hybrid positioning in complex indoor environments, has become a research hotspot.

Indoor scene identification depends on environmental conditions and signal conditions. The map, spatial structure, topological relationship and other information contained in the scene constitute the environmental conditions, while the rich acoustic, optical, electrical, magnetic and other information constitute the signal conditions. Existing research (Afif et al., 2020; Labinghisa and Lee, 2021; Guo et al., 2018; Miao et al., 2021) mainly focuses on using deep learning algorithms to extract and train image features in complex indoor environments, or on integrating wireless signals and barometric signals (Alameer et al., 2019; Luo et al., 2015) to achieve scene classification and identification. Deep learning algorithms with different structures have high requirements for the quantity, quality, transmission, and computational resources of images, making it difficult to deploy on existing terminals, and real-time acquisition of scene identification results also faces challenges. Currently, WiFi and Bluetooth devices are widely deployed in indoor environments to emit wireless signals in support of the internet of things, and their signals are influenced by the environment during propagation, exhibiting phenomena such as shadowing, fading, and multipath effects (Yassin et al., 2017). These characteristics cause signals to exhibit different features in different scenes, thereby providing a basis for scene identification methods based on wireless signals. However, existing devices often use omnidirectional antennas to increase signal coverage. The signal characteristics, especially the signal

strength, in physically close and adjacent scenes are relatively similar, which can lead to misidentification in some special scenarios, thereby reducing the accuracy of scene identification.

In response to the above issues, the paper proposed an indoor intelligent scene identification algorithm based on spatial topological constraints to improve scene identification accuracy, while also considering the efficiency of algorithm. Based on this algorithm, an intelligent scene identification system was developed to assist indoor positioning and improve positioning accuracy. Our contributions can be summarized as follows:

- 1) To improve the training efficiency and consider the accuracy of scene identification, a Naive Bayes (NB) classifier was adopted to train and classify the wireless signal strength data, thereby constructing a scene identification algorithm.
- 2) Based on the spatial entity attributes of indoor scenes, the topological relationships between scenes were analyzed to construct a topological relationship adjacency matrix and adjacency list, assisting in identification of adjacent scenario units.
- 3) A scene intelligent identification system centered on the scene identification algorithm and topological relationship constraints is proposed, establishing an online scene identification system to achieve real-time scene identification.

The rest of this paper is organized as follows. Section 2 is about the methods of the proposed algorithm and the schema of the developed system. Section 3 describes the experiments and analyses the results. Then the conclusions are presented in Section 4.

## 2. Methods

### 2.1 Naïve Bayes Classifier

Indoor scenes are composed of various scenario units. (Sun et al., 2015) had subdivided the indoor environments into narrow tunnels, small region, and large areas according to interior space

structure. These scenario units are indivisible, and the complex indoor scenes are composed of a combination of the three types of scenario units. Scene identification is essentially the process of learning and classifying wireless signals in different spatial environments. With the rapid development of artificial intelligence (AI) technology, a series of excellent machine learning algorithms have emerged, such as NB, Decision Tree (DT), Random Forest (RF), Support Vector Machine (SVM), and Artificial Neural Networks (ANN). These algorithms have their own advantages and have been widely used in various fields. The NB algorithm is a classification algorithm based on Bayes' theorem and the assumption of attribute independence. It has the characteristics of being simple to implement and computationally efficient, making it suitable for the real-time identification of scenes. Due to the widely deployment of Wi-Fi and Bluetooth devices in indoor environments, the wireless signals from these devices are mutually independent and do not interfere with each other. Therefore, this paper chooses the NB classifier to learn and classify the received signal strength (RSS) of Wi-Fi and Bluetooth in each scenario unit to achieve scene identification in indoor environments.

Given a sample dataset  $D = \{x_1, x_2, \dots, x_m\}$ , where each sample  $x_i = \{x_{i,1}, x_{i,2}, \dots, x_{i,d}\}$  is a vector of  $d$  attributes, and the class labels are  $y = \{c_1, c_2, \dots, c_N\}$ , meaning that the dataset  $D$  can be divided into  $N$  categories. Based on Bayes' theorem, the posterior probability of a sample can be expressed as follows:

$$P(c|x_i) = \frac{P(c)P(x_i|c)}{P(x_i)} \quad (1)$$

where  $P(c)$  is the prior probability of class  $c$ ,  $P(x_i|c)$  is the probability of the sample  $x_i$  given that the class is  $c$ ,  $P(c)$  is the total probability of the sample  $x_i$  and is considered to be same for all possible classes.

Given the assumption of attribute independence,  $P(c|x_i)$  can be approximately simplified to the following expression:

$$P(c|x_i) = \frac{P(c)}{P(x_i)} \prod_{j=1}^d P(x_{i,j}|c) \quad (2)$$

where  $x_{i,j}$  represents the value of the sample  $x_i$  on the  $j$ -th attribute and  $P(x_{i,j}|c)$  refers to the probability of  $j$ -th attribute under class  $c$ .

The class of a sample can be inferred by utilizing the maximum likelihood estimation method as expressed in equation (3).

$$h_{nb}(x_i) = \arg \max_{c \in y} P(c) \prod_{j=1}^d P(x_{i,j}|c) \quad (3)$$

According to the analysis of equations (1)-(3), the probabilities  $P(c)$  and  $P(x_{i,j}|c)$  are necessary to obtain to classify the sample  $x_i$ .

Since the strength of wireless signals is a discrete value, when the NB classifier is applied to the training of RSSI, the probability  $P(c)$  can be estimated using the following equation:

$$P(c) = \frac{|D_c|}{|D|} \quad (4)$$

where  $|D_c|$  is the number of samples class  $c$ ,  $|D|$  is the total number of samples. The probability  $P(x_{i,j}|c)$  can be expressed as:

$$P(x_{i,j}|c) = \frac{|D_{c,x_{i,j}}|}{|D_c|} \quad (5)$$

where  $|D_{c,x_{i,j}}|$  is the size of the subset  $D_c$  for  $j$ -th attribute.

Signal will fluctuate caused by temporal and spatial variations, it is not possible to capture all discrete values during the data training phase. Therefore, the signal strength values can be treated as continuous and assumed to follow a Gaussian normal distribution. The probability  $P(x_{i,j}|c)$  can be expressed as follows:

$$P(x_{i,j}|c) = \frac{1}{\sqrt{2\pi}\sigma_{c,j}} \exp\left(-\frac{(x_{i,j} - \mu_{c,j})^2}{2\sigma_{c,j}^2}\right) \quad (6)$$

where  $\mu_{c,j}$  and  $\sigma_{c,j}^2$  are respectively the mean and variance of the class  $c$  on the  $j$ -th attribute.

Once you had the training information of  $P(c)$  and  $P(x_{i,j}|c)$ , the collected RSSI could be used to determine the current user's scene in real-time according to equation (3). Therefore, the process of scene identification based on the NB algorithm can be summarized as follows:

Step 1: In an indoor environment, the scene was first divided into scenario units. Within each scenario unit, random walking was performed to collect Wi-Fi and Bluetooth signal strengths along with the corresponding MAC addresses, which were then compiled into a training dataset  $D$ . The data was stored at a rate of one second per entry to form the training dataset. Each sample's attribute corresponded to a unique MAC address, and each scenario was assigned a class label. The form of the dataset  $D$  can be expressed as follows.

Scenario unit	Mac(1)	Mac(2)	...	Mac(M)
$c_1$	$RSS_{c_1,1}$	$RSS_{c_1,2}$	...	$RSS_{c_1,m}$
$c_2$	$RSS_{c_2,1}$	$RSS_{c_2,2}$	...	$RSS_{c_2,m}$
$\vdots$	$\vdots$	$\vdots$	$\ddots$	$\vdots$
$c_N$	$RSS_{c_N,1}$	$RSS_{c_N,2}$	...	$RSS_{c_N,m}$

Table 1. The form of the dataset  $D$

Step 2: Based on the training data set  $D$ , the prior probabilities  $P(c)$  of each class were calculated and stored according to equation (4);

Step 3: Based on the data set  $D_c$ , calculated the mean  $\mu_{c,j}$  and variance  $\sigma_{c,j}^2$  of the  $j$ -th attribute respectively;

Step 4: Repeated steps 2 and 3 to complete the training of the dataset.

Step 5: When performing real-time scene identification, real-time signal strength data is collected. Then the probability of each scene was calculated, and the scene with the highest probability was returned as the identification result according to Equation (3).

## 2.2 The construction of spatial topology

Topological relationships are spatial relationships between spatial entities that do not consider metrics and direction. In the Geometry Information System (GIS), the description of topological relationships primarily involves three basic elements, namely: nodes, arcs, and polygons. These three basic elements correspond to the points, lines and surfaces in the space entity one by one. In the field of indoor positioning, narrow tunnels, small region, and large areas all have spatial extents, which can be understood as polygon elements. The relationship between scenario units only needs to consider the topological relationship between polygon elements. Therefore, the topological relationships between indoor scene units are limited to two types: adjacency and separation.

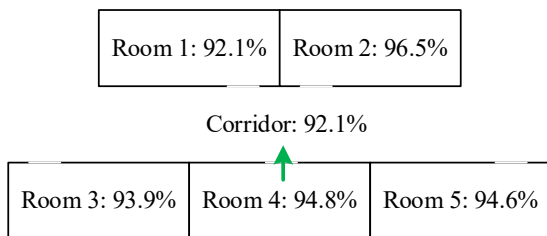


Figure 1. Example of spatial topological relationships assisting scene identification

In Figure 1, the scenario includes a total of 5 rooms and 1 corridor. Although each room is adjacent to the others, they are not interconnected, and each room is adjacent to the corridor. Topological relationship tables can be established between the rooms and the corridor in two forms: one is an adjacency matrix between the rooms and the corridor as shown in Table 2, which represents the connectivity between various scenes; the other is an adjacency list for the rooms and the corridor as shown in Table 3, which indicates the adjacent scene units for each scene. To prevent the table content from overflowing, Rooms 1 ~ 5 are abbreviated as R1 ~ R5.

Scenario	R1	R2	R3	R4	R5	Corridor
R1	1	0	0	0	0	1
R2	0	1	0	0	0	1
R3	0	0	1	0	0	1
R4	0	0	0	1	0	1
R5	0	0	0	0	1	1
Corridor	0	0	0	0	0	1

Table 2. Adjacency matrix between rooms and corridor

Scenario	Adjacency Unit
R1	R1, R2, Corridor
R2	R2, R1, Corridor
R3	R3, R4, Corridor
R4	R4, R3, R5, Corridor
R5	R5, R4, Corridor
Corridor	Corridor, R1, R2, R3, R4, R5

Table 3. Adjacency list between rooms and corridor

In Figure 1, the green arrow indicated that the user was at the entrance of room 4. When the user moved from Room 4 towards the corridor, the probability of identifying Room 2 was the highest. However, according to the adjacency list between rooms and the corridor from Table 3, it could be observed that Room 2 was not listed among the adjacent units of Room 4. Additionally, by traversing the adjacent units of Room 4, it was determined that the probability of the corridor is the highest. By

examining the adjacency matrix from Table 3, it was found that the connectivity value between Room 4 and the corridor was 1, indicating that Room 4 was adjacent to the corridor. Therefore, it could be inferred that the next scene unit was the corridor with an identification probability of 94.8%.

This flowchart described the process of assisting scene identification by leveraging the spatial topological relationships within an indoor environment. The process steps were summarized as follows:

Step 1: Performed scene identification using a NB classifier and output the identification probabilities for each scene.

Step 2: Selected the scene with a higher probability as a preliminary candidate result, then checked the current scene's adjacency list to determine whether the candidate result was adjacent to the current scene.

Step 3: If it was not an adjacent relationship, returned to Step 2 to select the next scene with a higher probability.

Step 4: If it was an adjacent relationship, then check the adjacency matrix to determine if there was connectivity.

Step 5: If there was connectivity between two scenes, output the result; if there was no connectivity, returned to Step 2 to continue the assessment, and repeated this process until the final scene identification result was outputted.

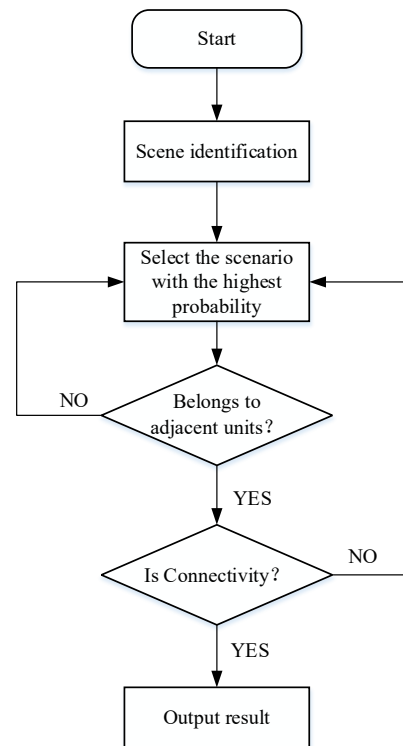


Figure 2. Flow chart of spatial topological relationship assisting scene identification

## 2.3 Online scene identification system

An intelligent scene identification system centered on the scene identification algorithm and topological relationship constraints was proposed. The solution diagram was shown in Figure 3.

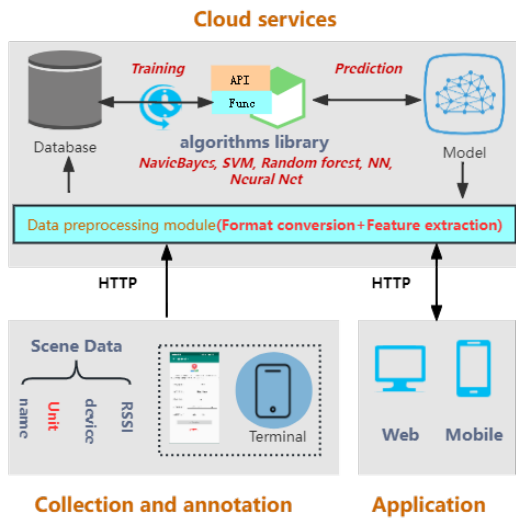


Figure 3. Construction scheme of scene identification system

The construction scheme for the scene identification system broken down the scene identification process into three subsystems, covering the main processes of scene data collection, training, and identification. The three subsystems were as follows: data collection and annotation system, the scene identification cloud service, and the online application.

The data collection and annotation system collected and uploaded current scene data through the HyperText Transfer Protocol (HTTP). The scene data mainly included the names of places, scene units, device names, and feature data. Scene units required manual participation for annotation. The scene identification cloud service was responsible for receiving, processing, storing, training, and generating predictive models for scene identification data. The data processing module included feature extraction and format conversion functions, which were responsible for processing the uploaded scene identification data into vectors, compressing and storing data in the scene identification database for training. The core of the cloud service was the machine learning algorithm library, which included many algorithms such as NB, SVM, RF, DT, and NN. It could choose the appropriate classifier based on the signal type, and periodically retrieved data from the scene identification database for offline learning and updates the predictive model. The online application was responsible for the collection and upload of real-time signal data, waiting for scene identification results and display it.

The online scene identification system decouples the scene identification process according to data collection, processing, and verification, reducing the complexity and enhancing the stability of the system. It also uses a terminal-cloud collaborative approach to achieve the development of the system, making full use of the computing and storage resources of the terminal and cloud.

### 3. Experiments and Analysis

#### 3.1 Environmental Setup

The indoor scene identification experimental site was located at the C7 AI Experimental Field of the 54th Research Institute of the China Electronics Corporation Group. The experimental site, as shown in Figure 4, was 24.92 meters long and 27.49 meters wide. The site was divided into three floors, each with a

different structural layout. The first floor was a lobby with a rectangular atrium structure connecting to the second and third floors. The second floor of the experimental field consisted of a rectangular corridor, the interior walls of which were entirely made of tempered glass. Along one side of the corridor, there were three small rooms. The corridor and rooms contained objects such as tables, chairs, and equipment. The third floor had three elongated room areas.

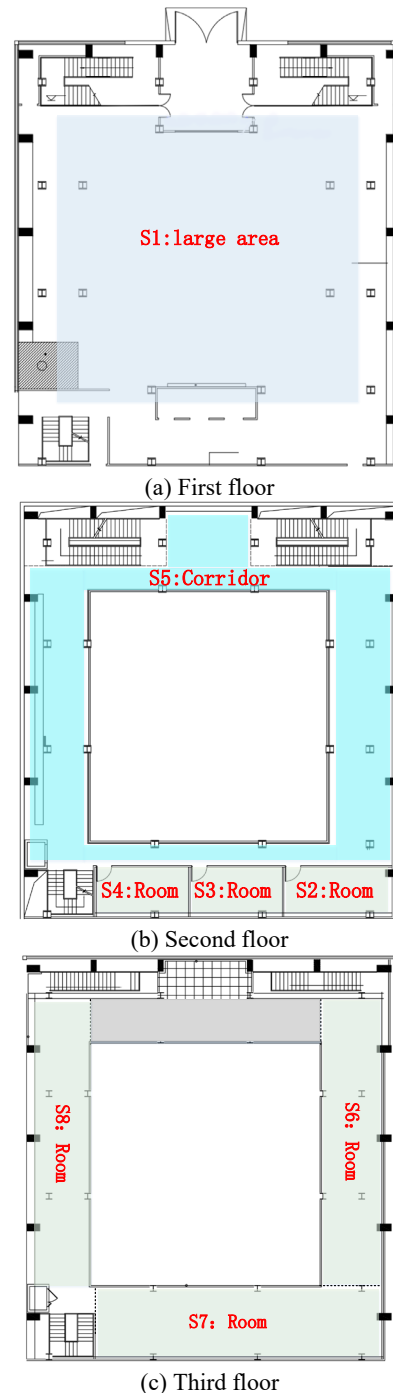


Figure 4. Spatial distribution of each scene

The entire experimental site was divided into 8 scene units, represented as S1 to S8. Each scenario unit had already been labeled in Figure 4. There were Wi-Fi routers and Bluetooth base stations specifically installed for indoor positioning experiments. Due to the influence of the glass curtain walls, the

propagation of Wi-Fi and Bluetooth wireless signals was severely affected by multipath effects. Each scene unit was within the coverage area of Wi-Fi and Bluetooth wireless signals.

Wi-Fi and Bluetooth signals were collected for scene data training by utilizing crowdsourced information collection software. The data included the name of the experimental site, the scene name, and the device name. Users walked freely in each scene, trying to cover the entire area of the scene with their movement. Data was collected for 400 seconds in each scene to form a training dataset. Additionally, another 400 seconds of data was collected in each scene to serve as test data. There were a total of 3,295 training data entries and 3,289 test data entries. These training data were input into many classifiers for training and testing. The results from each were statistically analyzed and compared.

### 3.2 Environmental Results and Analysis

Before the data were input into the classifiers for training and testing, preprocessing of the data is required. This mainly included the removal of useless data. Useless data primarily consisted of noise within the entire training and testing datasets,

which might be interference caused by other users' mobile phones with Bluetooth or Wi-Fi hotspots enabled during the data collection process. Additionally, due to the particularity of the signal strength data type, 0-value data in the dataset was replaced with the value of -115, indicating that the user is either far away or not receiving valid RSS. After the data preprocessing, the number of attributes in the dataset was reduced from 202 to 189, indicating that 13 attribute data belong to the invalid data.

In addition to using the NB algorithm as a scene identification training classifier, other machine learning methods such as DT, KNN, linear SVM, and NN were also compared using the same dataset. The training time and scene identification accuracy of each method were compared in Tables 4 and 5.

Method	Training time/s	Overall accuracy
NB	1.278	97.1%
DT	0.558	63.7%
KNN	1.241	90.6%
Linear SVM	3.152	98.1%
NN	2.639	97.2%

Table 4. Performance of various classifiers

Method	S1	S2	S3	S4	S5	S6	S7	S8
NB	99.7%	98.3%	92.3%	100.0%	99.3%	96.7%	95.3%	88.0%
DT	19.7%	100%	0.0	100%	97.2%	11.4%	59.9%	19.7%
KNN	66.6%	99.0%	93.6%	99.0%	95.2%	95.3%	96.7%	65.6%
Linear SVM	100.0%	100.0%	94.3%	99.3%	99.9%	94.0%	97.3%	64.3%
NN	98.7%	97.0%	95.7%	99.7%	99.0%	95.3%	93.6%	93.3%

Table 5. The identification accuracy of each scene with different classifiers

From the Table 4 and Table 5, it could be observed that the method DT exhibited relatively poor performance in both overall scene identification and individual scene identification rates. The linear SVM achieved the highest accuracy in scene identification and maintained a high level of accuracy across various scenarios, although it had the longest training time. The classification performance of the NN classifier was close to the NB classifier in terms of accuracy, but there was a significant difference in training time. The training time of the KNN classifier was comparable to the NB classifier but its scene identification accuracy was 90.6%, which is lower than the

97.1% of the NB classifier. Due to the deployment of Wi-Fi and Bluetooth base stations on the first and second floors, the signal characteristic data fluctuated more noticeably on these floors across different scenes. Consequently, the identification accuracy for scenarios 1 to 5 were higher than for scenarios 6 through 8 based on various positioning methods. In summary, the scene identification algorithm based on the NB method kept a balance between identification accuracy and training efficiency, demonstrating the best overall performance in this environment.

Accuracy	S1	S2	S3	S4	S5	S6	S7	S8
S1	99.7%	0.0	0.0	0.0	0.3%	0.0	0.0	0.0
S2	0.0	98.3%	1.7%	0.0	0.0	0.0	0.0	0.0
S3	0.0	7.7%	92.3%	0.0	0.0	0.0	0.0	0.0
S4	0.0	0.0	0.0	100.0%	0.0	0.0	0.0	0.0
S5	0.5%	0.0	0.0	0.0	99.3%	0.1%	0.0	0.1%
S6	0.0	0.0	0.0	0.0	0.7%	97.0%	2.3%	0.0
S7	0.0	0.0	0.0	0.0	0.0	3.0%	95.3%	1.7%
S8	0.3%	0.0	0.0	0.0	4.0%	0.0	7.7%	88.0%

Table 6. Scene identification confusion matrix of Naive Bayes classifier

Table 6 displayed the confusion matrix for scene identification based on the NB classifier, where the first columns represented the true class of the scenarios, and the rows indicated the predicted categories of the scenarios. From Table 6, it could be observed that spatially adjacent scenes were more susceptible to misidentification. For example, between Scene 2 and Scene 3, which were two adjacent rooms, misidentifications might occur. Scenes 5, 6, 7, and 8 also exhibited this issue.

To suppress such misidentifications, constraints based on the topological relationships between scenes were utilized. A

topological relationship table between scenes was established according to their spatial distribution. According to the scenes depicted in Figure 4, the adjacency matrix for Scenes 1 to 8 was constructed as shown in Table 7.

In Table 7, the value 1 indicated that there was an adjacency relationship between the scenes and they were connectivity while the value 0 indicated that there was no connectivity between scenes. For first row, Scene 1 was the lobby on the first floor, and Scene 5 is the corridor on the second floor. According to the spatial relationship, Scene 1 was adjacent to Scene 5.

Although Scene 1 has an overlapping area with Scene 2 in the planar projection, they were in a separated relationship. The

establishment of connectivity between other scenes was done in the same manner.

Accuracy	S1	S2	S3	S4	S5	S6	S7	S8
S1	1	0	0	0	1	0	0	0
S1	0	1	0	0	1	0	0	0
S1	0	0	1	0	1	0	0	0
S1	0	0	0	1	1	0	0	0
S1	1	1	1	1	1	1	0	0
S1	0	0	0	0	1	1	1	0
S1	0	0	0	0	0	1	1	1
S1	0	0	0	0	0	0	1	1

Table 7. Adjacency matrix from scene 1 to 8

Table 8 was the adjacency list for the scenes, which was used to look up the adjacent units of each scene.

Scenario	Adjacency Unit
S1	S1, S5
S2	S2, S3, S5
S3	S3, S2, S4, S5
S4	S4, S3, S5
S5	S5, S1, S2, S3, S4, S6
S6	S6, S5, S7
S7	S7, S6, S8
S8	S8, S7

Table 8. Adjacency list between from scene 1 to 8

According to the process of scene identification, the topological relationships between scenes were inspected and constrained during real-time scene identification. Based on the topological relationship constraints, the confusion matrix for the identification of each scene was demonstrated in Table 9. From Table 9, it could be seen that the identification accuracy for each scene units had been enhanced by utilizing the topological relationship constraints except for scene 7. The misidentification accuracy between the two adjacent scenes, Scene 6 and Scene 8, had not decreased. This phenomenon was due to the fact that Scene 7 was connected and adjacent to both Scene 6 and Scene 8, fulfilling the topological constraint conditions, which results in the scene constraint became ineffective in this case.

Accuracy	S1	S2	S3	S4	S5	S6	S7	S8
S1	100.0%	0.0	0.0	0.0	0.0	0.0	0.0	0.0
S2	0.0	100.0%	0.0	0.0	0.0	0.0	0.0	0.0
S3	0.0	0.0	100.0%	0.0	0.0	0.0	0.0	0.0
S4	0.0	0.0	0.0	100%	0.0	0.0	0.0	0.0
S5	0.3%	0.0	0.0	0.0	99.6%	0.1%	0.0	0.0
S6	0.0	0.0	0.0	0.0	0.7%	97.3%	2.0%	0.0
S7	0.0	0.0	0.0	0.0	0.0	3.0%	95.3%	1.7%
S8	0.0	0.0	0.0	0.0	0.0	0.0	9.0%	91.0%

Table 9. Scene identification confusion matrix of Naive Bayes classifier

For the other scenes, the process began by checking the topological relationships. If no adjacency was found, the procedure described in Figure 2 was followed. The system continues to compare the probability values of the remaining scenes, selecting the scene with the highest probability value as the candidate result. Then, it conducted another topological relationship check. This cycle continued until the conditions were met, and the final scene identification result was outputted. With the assistance of topological relationship constraints in scene identification, the overall accuracy of the 8 scenes was 98.2%, which had an improvement of 1.1% compared to the accuracy 97.1% of original NB classifier. We could conclude that the accuracy of scene identification had been improved to a certain extent by incorporating topological relationship constraints.

#### 4. Conclusion

Researching indoor scene identification helps to enhance the scene change perception capability of indoor positioning, improving the intelligence and effectiveness of the system. To address the issue of adjacent scenes being easily confused in identification and considering the difficulty and real-time requirements of algorithm implementation, this paper proposed an indoor intelligent scene identification system based on

spatial topological relationship constraints. This technical solution employed an NB classifier for scene training and classification, and incorporated spatial topological relationships to constrain and optimize scene identification. A scene intelligent identification system centered on the scene identification algorithm and topological relationship constraints was also developed. The experimental results indicated that the scene identification method based on spatial topological relationship constraints could effectively improve identification accuracy. However, the spatial topological relationships were only used for constraints and did not take effect in some special cases. In the future, we will focus on researching the connection between spatial topological relationships and knowledge graphs to enhance their role in intelligent scene identification.

#### References

- Afif, M., Ayachi, R., Said, Y., and Atri, M., 2020. Deep Learning Based Application for Indoor Scene Recognition, *Neural Process. Lett.*, 51(2827-2837), 10.1007/s11063-020-10231-w.
- Alameer, A., Degenaar, P., and Nazarpour, K., 2020. Context-Based Object Recognition: Indoor Versus Outdoor

Environments, *Computer Vision Conference (CVC)*, Las Vegas, NV, Apr 25-26, 473-490, 10.1007/978-3-030-17798-0\_38.

Guo, W., Wu, R., Chen, Y. H., and Zhu, X. Y., 2018. Deep Learning Scene Recognition Method Based on Localization Enhancement, *Sensors*, 18(20), 10.3390/s18103376.

Labinghisa, B. and Lee, D. M., 2021. A Deep Learning based Scene Recognition Algorithm for Indoor Localization, *3rd International Conference on Artificial Intelligence in Information and Communication (IEEE ICAIIC)*, South Korea, Apr 13-16, 167-170, 10.1109/icaaic51459.2021.9415278.

Luo, D., Luo, H. Y., and Chen, Z. L., 2015. An Indoor Scene Recognition Algorithm based on Pressure Change Pattern, *8th International Conference on Intelligent Computation Technology and Automation (ICICTA)*, Nanchang, PEOPLES R CHINA, Jun 14-15, 149-152, 10.1109/icicta.2015.46.

Miao, B., Zhou, L. G., Mian, A. S., Lam, T. L., and Xu, Y. S., 2021. Object-to-Scene: Learning to Transfer Object Knowledge to Indoor Scene Recognition, *IEEE/RSJ International Conference on Intelligent Robots and Systems (IROS)*, Electr Network, Sep 27-Oct 01, 2069-2075, 10.1109/iros51168.2021.9636700.

Obeidat, H., Shuaieb, W., Obeidat, O., and Abd-Alhameed, R., 2021. A Review of Indoor Localization Techniques and Wireless Technologies, *Wirel. Pers. Commun.*, 119(289-327), 10.1007/s11277-021-08209-5.

Sun, J., Fu, Y. L., Tan, L., and Li, S. G., 2015. A Survey and Application of Indoor Positioning Based on Scene Classification Optimization, *12th IEEE Int Conf Ubiquitous Intelligence & Comp/12th IEEE Int Conf Autonom & Trusted Comp/15th IEEE Int Conf Scalable Comp & Commun & Associated Workshops/IEEE Int Conf Cloud & Big Data Comp/IEEE Int Conf Internet People*, Beijing, PEOPLES R CHINA, Aug 10-14, 1558-1562, 10.1109/UIC-ATC-ScalCom-CBDCCom-IoP.2015.282.

Yassin, A., Nasser, Y., Awad, M., Al-Dubai, A., Liu, R., Yuen, C., Raulefs, R., and Aboutanios, E., 2017. Recent Advances in Indoor Localization: A Survey on Theoretical Approaches and Applications, *IEEE Commun. Surv. Tutor.*, 19(1327-1346), 10.1109/comst.2016.2632427.